# Regulation of *Drosophila* IAP1 degradation and apoptosis by *reaper* and *ubcD1*

**Hyung Don Ryoo\*, Andreas Bergmann†, Hedva Gonen‡, Aaron Ciechanover‡ and Hermann Steller\*§**

*\*Howard Hughes Medical Institute, Strang Laboratory of Cancer Research, The Rockefeller University Box 252, 1230 York Ave. New York, NY 10021, USA*
*†Department of Biochemistry and Molecular Biology, University of Texas, M.D. Anderson Cancer Center, Houston, TX 77030, USA*
*‡Department of Biochemistry, Faculty of Medicine, Technion – Israel Institute of Technology, Haifa 31096, Israel*
*§e-mail: steller@mail.rockefeller.edu*

focus on *apoptosis*

**Cell death in higher organisms is negatively regulated by Inhibitor of Apoptosis Proteins (IAPs), which contain a ubiquitin ligase motif, but how ubiquitin-mediated protein degradation is regulated during apoptosis is poorly understood. Here, we report that *Drosophila melanogaster* IAP1 (DIAP1) auto-ubiquitination and degradation is actively regulated by Reaper (Rpr) and UBCD1. We show that Rpr, but not Hid (head involution defective), promotes significant DIAP1 degradation. Rpr-mediated DIAP1 degradation requires an intact DIAP1 RING domain. Among the mutations affecting ubiquitination, we found *ubcD1*, which suppresses *rpr*-induced apoptosis. UBCD1 and Rpr specifically bind to DIAP1 and stimulate DIAP1 auto-ubiquitination *in vitro*. Our results identify a novel function of Rpr in stimulating DIAP1 auto-ubiquitination through UBCD1, thereby promoting its degradation.**

In all metazoans, programmed cell death, or apoptosis, is essential for proper development and the maintenance of body homeostasis[1]. Apoptosis is triggered by caspases, members of a cysteine protease family that, when activated, trigger the distinct cellular changes observed in many, if not all, dying cells[2]. The decision to trigger apoptosis depends on the balance between factors that activate caspases and those that inhibit them. IAPs are negative regulators of apoptosis that bind to caspases and inhibit their activity[3]. Consistent with this function, inhibition of IAPs has been found to be an important step, resulting in caspase activation in mammals and *Drosophila*.

The important function of IAPs is evident from genetic studies in *Drosophila*. *diap1* is encoded by the *thread* (*th*) locus. In loss-of-function *diap1* mutants, apoptosis occurs in virtually all cells during early stages of embryogenesis[4]. The anti-apoptotic function of *diap1* is blocked by proteins such as Rpr, Hid and Grim[5–7], which share an 8-amino-acid amino-terminal peptide motif (RHG motif). This RHG motif binds to the DIAP1 baculoviral IAP repeat (BIR) domains[8], which are evolutionarily conserved regions found in all IAPs. *diap1* alleles with mutations in BIR domains suppress *hid*- and *rpr*-induced cell death[6,7]. The essential function of RHG proteins in apoptosis is evident from the studies of *Drosophila* *Df(3L)H99*−/− embryos, which lack the *hid*, *rpr* and *grim* genes, and in which no apoptosis occurs[9]. IAP inhibition by RHG proteins is similarly crucial during apoptosis in mammals; the mitochondrially localized mammalian RHG proteins Smac/DIABLO and HtrA2 are released into the cytoplasm after apoptotic stimuli and relieve caspase inhibition by IAPs[10–15].

IAPs, including DIAP1, contain a conserved RING finger domain that functions as a ubiquitin ligase[16]. Ubiquitin ligases recruit E2 ubiquitin-conjugating enzymes, facilitating transfer of ubiquitin to substrate proteins and thereby tagging them for proteasome-mediated degradation. IAPs can mediate both auto-ubiquitination and ubiquitination of caspases, and their ubiquitination activity is actively regulated[17–19]. For example, glucocorticoid treatment of thymocytes stimulates IAP auto-ubiquitination and degradation before the onset of apoptosis[19]. However, the molecules
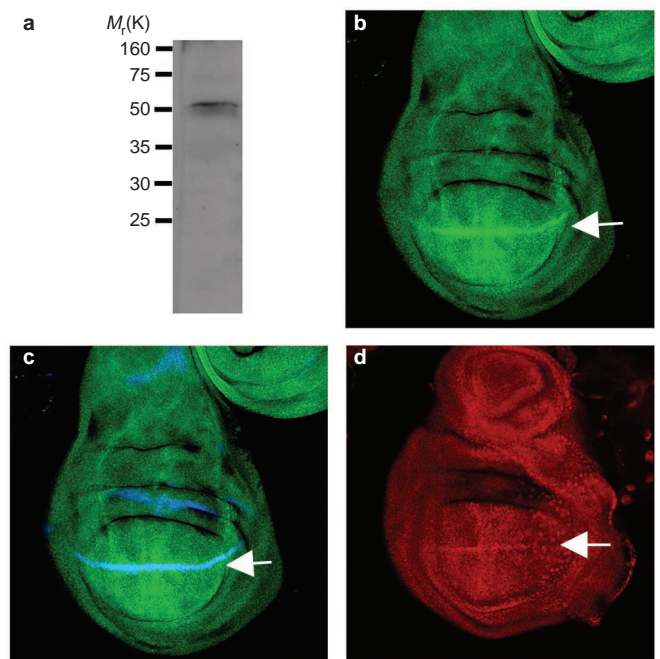


**Figure 1 Expression of DIAP1 protein and *diap1* enhancer trap in wing imaginal discs. a,** An anti-DIAP1 western blot of embryo extracts detects a single band with a relative molecular mass ($M_r$) of approximately 50,000 (50K), the predicted size of the *diap1* gene product. **b,c,** Whole-mount anti-DIAP1 labelling of late third instar larval wing imaginal discs, producing a distinctive pattern of anti-DIAP1 labelling (**b**, green). The stripe of cells with higher levels of DIAP1 (arrow) coincides with the D–V boundary, as demonstrated by costaining with the D–V marker *wg-lacZ* (**c**, blue). **d,** Anti-β-galactosidase labelling (red) of the *diap1-lacZ* (*th[j5c8]*) line produces a pattern similar to the anti-DIAP1 labelling in **b** and **c**.
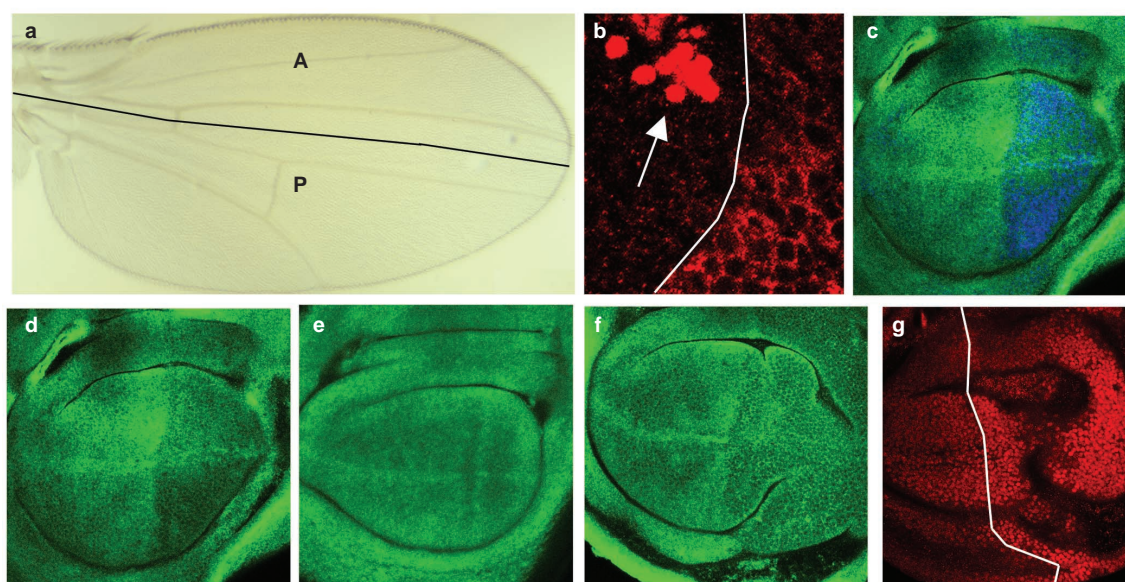
Figure 2 *rpr* induces post-transcriptional downregulation of DIAP1. With the exception of **a**, anterior is to the left and posterior to the right. The A–P boundary is outlined in **a**, **b** and **g**. **a**–**d**, *rpr* and *p35* were ectopically expressed in the wing imaginal disc posterior compartment. Genotype, *UAS-rpr*; *UAS-p35/en-Gal4*. **a**, p35 completely blocks *rpr*-induced cell death and flies develop wings with minimal defects. Anterior (A) is up and posterior (P) down. **b**, In the anterior compartment, the CM1 antibody (red) intensely labels naturally dying cells (arrow). In the posterior compartment, all cells are labelled with CM1, but staining was confined to the cyto-plasm. **c,d**, Wing imaginal discs labelled with the anti-DIAP1 antibody (green) show reduced DIAP1 levels in the posterior compartment. The posterior compartment is marked by double labelling with the anti-EN antibody (**c**, blue). **e**, Expression of *p35* alone does not affect DIAP1 levels (green). Genotype, *UAS-p35/en-Gal4*. **f**, *hid* and *p35* were co-expressed in the posterior compartment and labelled with the anti-DIAP1 antibody (green). Genotype, *UAS-hid*; *UAS-p35/en-Gal4*. Compared to **c** and **d**, *hid* does not induce an obvious reduction of DIAP1 levels. **g**, *diap1-lacZ* (*thi5c8*) expression (red) is higher in the posterior compartment, where *rpr* is expressed. This indicates that the observed reduction of DIAP1 in **c** and **d** is post-transcription-al. Genotype, *UAS-rpr/+*; *UAS-p35/en-Gal4*; *diap1-lacZ* (*thi5c8*)/+.

responsible for regulating IAP degradation have not yet been identified.

In this study, we have used the genetic tools of *Drosophila* to address how DIAP1 levels are regulated. We show that expression of *rpr* stimulates DIAP1 ubiquitination and degradation. Moreover, DIAP1 promotes its own ubiquitination through its RING domain and UBCD1, a ubiquitin-conjugating enzyme. We propose that, in addition to binding DIAP1, certain RHG proteins have the additional ability to stimulate DIAP1 degradation, thereby promoting apoptosis.

## Results

**DIAP1 expression pattern.** To investigate how DIAP1 is regulated, we generated a polyclonal antibody against recombinant DIAP1 protein that detects a single band on western blots (Fig. 1a). In whole-mount staining of larval imaginal discs, we noted that the amount of DIAP1 varied between some tissues. Notably, in wing imaginal discs, a strip of cells showed increased anti-DIAP1 labelling (Fig. 1b). These cells constitute the dorso–ventral (D–V) boundary, as demonstrated by double labelling with the *wingless* (*wg*)-*lacZ* marker[20] (Fig. 1c). Consistent with the anti-DIAP1 anti-body labelling pattern, imaginal discs from *thi5c8* animals, which have a P[lacZ] insertion in the 5′ untranslated region of the *diap1* transcription unit[4], showed stronger anti-β-galactosidase labelling along the D–V boundary (Fig. 1d). We conclude that in the wing imaginal disc, *thi5c8* P[lacZ] reporter expression reflects *diap1* tran-scription.

**Rpr induces post-transcriptional downregulation of DIAP1.** To determine if DIAP1 degradation is also regulated in *Drosophila*, we co-expressed *rpr* and the baculovirus *p35* caspase inhibitor[21] in the wing imaginal disc posterior compartment using the *engrailed* (*en*)-*Gal4* driver[22]. Expression of *p35* prevented *rpr*-expressing cells

from dying, and the resulting 'undead' cells enabled us to observe cellular changes downstream of *rpr*. Whereas animals expressing *rpr* alone died as embryos, those co-expressing *rpr* and *p35* survived to adulthood with largely normal wings (Fig. 2a). *rpr*-induced cell death was completely blocked by *p35*, as assayed by TUNEL stain-ing of wing imaginal discs (data not shown). We also labelled wing imaginal discs with the CM1 antibody, which detects activated cas-pase-3 in humans and cross-reacts with activated caspases in *Drosophila*[23,24]. In the control anterior compartment, sporadic apoptotic cells were intensely labelled with CM1 (Fig. 2b). In con-trast, all undead cells of the posterior compartment showed low but consistent levels of CM1 labelling (Fig. 2b). Whereas in apoptotic cells, CM1 labelling was detected throughout the cell body, in undead cells, CM1 labelling was detected only in the cytoplasm, indicating that the nuclear membrane was intact and cells were not dying.

Interestingly, cells expressing both *rpr* and *p35* had reduced anti-DIAP1 labelling, compared to the wild type cells of the anteri-or compartment (Fig. 2c,d). Expression of *p35* alone did not affect the amount of *diap1* expression (Fig. 2e). Unlike *rpr*, co-expression of *hid* and *p35* did not cause obvious DIAP1 downregulation (Fig. 2f). The different effects of *hid* and *rpr* on DIAP1 downregulation might partly account for the different cell killing properties report-ed previously[7,25,26].

The reduction in DIAP1 levels by Rpr was not caused by reduced transcription, as *diap1-lacZ* expression in *thi5c8* mutants actually increased in these cells (Fig. 2g). As Rpr can bind directly to DIAP1 (ref. 6), our result suggests that Rpr–DIAP1 complex for-mation triggers DIAP1 downregulation through a post-transcrip-tional mechanism and that this occurs independently of caspase activity.

**rpr induces DIAP1 degradation in a RING-domain-dependent manner.** A number of *diap1* mutant alleles exist that disrupt the
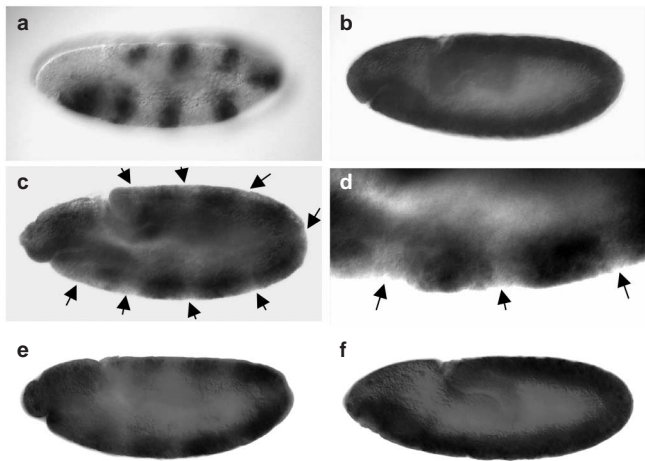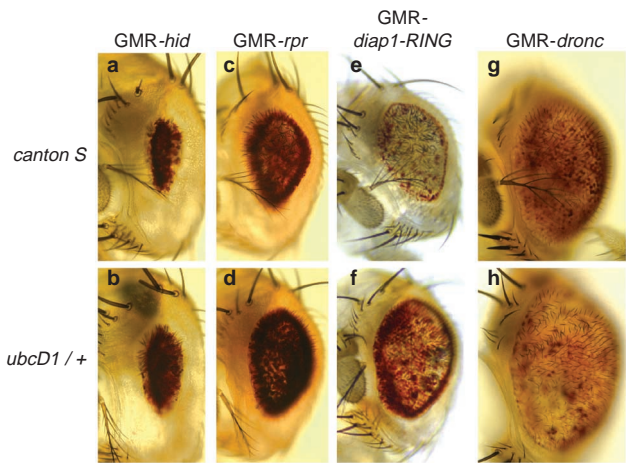
Figure 3 **rpr induced DIAP1 degradation is dependent on the RING domain.**
**a**, *prd-Gal4* expression pattern. Genotype, *prd-Gal4/ UAS-lacZ*. Anti-β-galactosidase staining of the embryo shows *lacZ* expression in a *prd*-like pattern. **b**, A wild type embryo stained with the anti-DIAP1 antibody. The DIAP1 protein is homogenously distributed. **c**, Expression of *rpr* reduces DIAP1 staining. Genotype, *UAS-rpr; prd-Gal4*. The domains of *rpr* expression and of reduced anti-DIAP1 staining match each other (see arrows and compare with the embryo in **a**). **d**, An enlarged view of the embryo in **c**. **e**, The degradation of DIAP1 is independent of caspases. Genotype, *UAS-rpr; UAS-p35; prd-Gal4*. Co-expression of the caspase inhibitor *p35* does not block *rpr*-induced DIAP1 downregulation. **f**, The degradation of DIAP1 in response to *rpr* expression requires the RING domain. Genotype, *UAS-rpr; prd-Gal4, diap1$^{33-1S}$/diap1$^{22-8S}$*. Expression of *rpr* in a RING mutant background fails to trigger DIAP1 degradation.



Figure 4 **Mutation in *ubcD1* dominantly suppresses cell killing induced by GMR-hid, GMR-rpr and GMR-diap1-RING.** Cell killing activity as visualized in adult eyes. Genotypes are as follows: *GMR-hid/+* (**a**), *GMR-hid/+; ubcD1$^{D73}$/+* (**b**), *GMR-rpr/+* (**c**), *GMR-rpr/+; ubcD1$^{D73}$/+* (**d**), *GMR-diap1-RING/+* (**e**), *GMR-diap1-RING/+; ubcD1$^{D73}$/+* (**f**), *GMR-Gal4/+; UAS-dronc/+* (**g**) and *GMR-Gal4/+; UAS-dronc/ubcD1$^{D73}$* (**h**). **a–d**, *ubcD1$^{-/+}$* partially suppresses the eye ablation phenotype of *GMR-hid* and *GMR-rpr*. **e**, *GMR-diap1-RING* induces eye pigment cell death. **f**, In a *ubcD1$^{-/+}$* background, pigment loss by *GMR-diap1-RING* is partially suppressed. **g**, *GMR-dronc* similarly induces pigment cell loss. **h**, However, *ubcD1$^{-/+}$* enhances the effect of *GMR-dronc*. This places *ubcD1* genetically downstream of *hid* and *rpr*, but not downstream of *dronc*.

RING domain of DIAP1 (refs 7,27). We used two such *diap1* mutant alleles, *diap1$^{33-1S}$* and *diap1$^{22-8S}$*, to address the requirement of the RING domain for *rpr*-dependent DIAP1 degradation.

Homozygous or *trans*-heterozygous combinations of these alleles are embryonic lethal, indicating that the RING domain provides an essential function for DIAP1 (ref. 7). Thus, we determined the effect of the RING finger mutations on *rpr*-dependent DIAP1 degradation in embryos. The protein distribution of DIAP1 was analysed in embryos that express *rpr* under the *prd-Gal4* driver (Fig. 3a,c). In wild type embryos, DIAP1 was homogenously distributed (Fig. 3b). However, if *rpr* expression was induced in a *prd*-like expression pattern, DIAP1 protein levels decreased in exactly those domains where *rpr* was expressed (Fig. 3c,d). Co-expression of *p35* did not affect the decrease of DIAP1 protein levels (Fig. 3e), suggesting that it occurs upstream and independently of caspase activation.

To address the importance of the RING domain for the decrease in DIAP1 levels, we expressed *rpr* in a RING domain mutant background using the *diap1$^{33-1S}$* and *diap1$^{22-8S}$* alleles. Under this experimental condition, *rpr* was no longer able to downregulate DIAP1 (Fig. 3f). These observations suggest that the reduction of DIAP1 by Rpr is caused by auto-ubiquitination-mediated protein degradation.

**ubcD1 promotes rpr- and hid-induced apoptosis, but not caspase-induced apoptosis.** GMR-*hid* and GMR-*rpr* animals ectopically express *hid* or *rpr* in the developing eye discs. Such expression triggers cell killing and is sensitive to the dosage of other cell-death-related genes, such as *diap1* (ref. 4). To identify additional factors that regulate DIAP1 auto-ubiquitination, we searched animals heterozygous for mutations in the ubiquitin pathway that enhanced or reduced GMR-*hid* or GMR-*rpr* induced cell killing (Table 1). We found several dominant enhancers of GMR-*rpr*, including *Pros26*, a

proteasome subunit[28], *fat facet*, a de-ubiquitinating enzyme[29] and *Drosophila bruce*, encoding a ubiquitin-conjugating enzyme (J. Agapite and H.S., unpublished observations). None of these mutations enhanced GMR-*hid*-induced apoptosis.

Mutations in genes that are required for Rpr-mediated DIAP1 degradation are expected to dominantly suppress GMR-*rpr*. We found only one such suppressor, *ubcD1*, also known as *effete*. *ubcD1* encodes a 147-amino-acid ubiquitin-conjugating enzyme that is similar to the mammalian ubcH5 class[30–32]. The dominant suppression of GMR-*hid* and GMR-*rpr* was observed with two independent alleles, *ubcD1$^{598}$* and *ubcD1$^{D73}$* (Fig. 4a–d). Interestingly, *ubcD1* was previously identified as a genetic interactor of *sina*, a gene encoding a RING domain with high sequence similarity to the DIAP1 RING domain[32]. To test if *ubcD1* interacted genetically with the RING domain of *diap1*, *ubcD1* flies were crossed to GMR-*diap1-RING* flies, which overexpress the carboxy-terminal part of DIAP1, including the RING domain. GMR-*diap1-RING* induces cell death and results in small eyes that lack pigment cells[4] (Fig. 4e). In *ubcD1$^{-/+}$* animals, the eye phenotype caused by GMR-*diap1-RING* was suppressed and more pigment cells survived (Fig. 4f).

The dominant suppression of GMR-*rpr*, GMR-*hid* and GMR-*diap1-RING* seems to be specific to *ubcD1*, as mutations in *less-wright* (*lwr*; a *ubc9* homologue) and *ubcD2* (a *ubc4* homologue) had no effect on GMR-*rpr*, GMR-*hid* or GMR-*diap1-RING* animals (Table 1). *ubcD2* has high sequence similarity to *ubcD1*, and both genes have been shown to functionally substitute for *ubc4* in yeast[30,33]. Therefore, our results indicate a striking level of specificity among similar ubiquitin-conjugating enzymes *in vivo*.

*hid* and *rpr* induce apoptosis through *dronc*, a *Drosophila* caspase-9 homologue[34,35]. GMR-*dronc* induces apoptosis during late pupal stages, which results in a loss of pigment cells within normal-sized eyes (Fig. 4g). We found that *ubcD1* did not dominantly suppress GMR-*dronc* activity, indicating that it functions downstream of *rpr*, but upstream of *dronc* (Fig. 4h). In fact, *ubcD1* slightly enhanced GMR-*dronc* activity, raising the possibility that Dronc
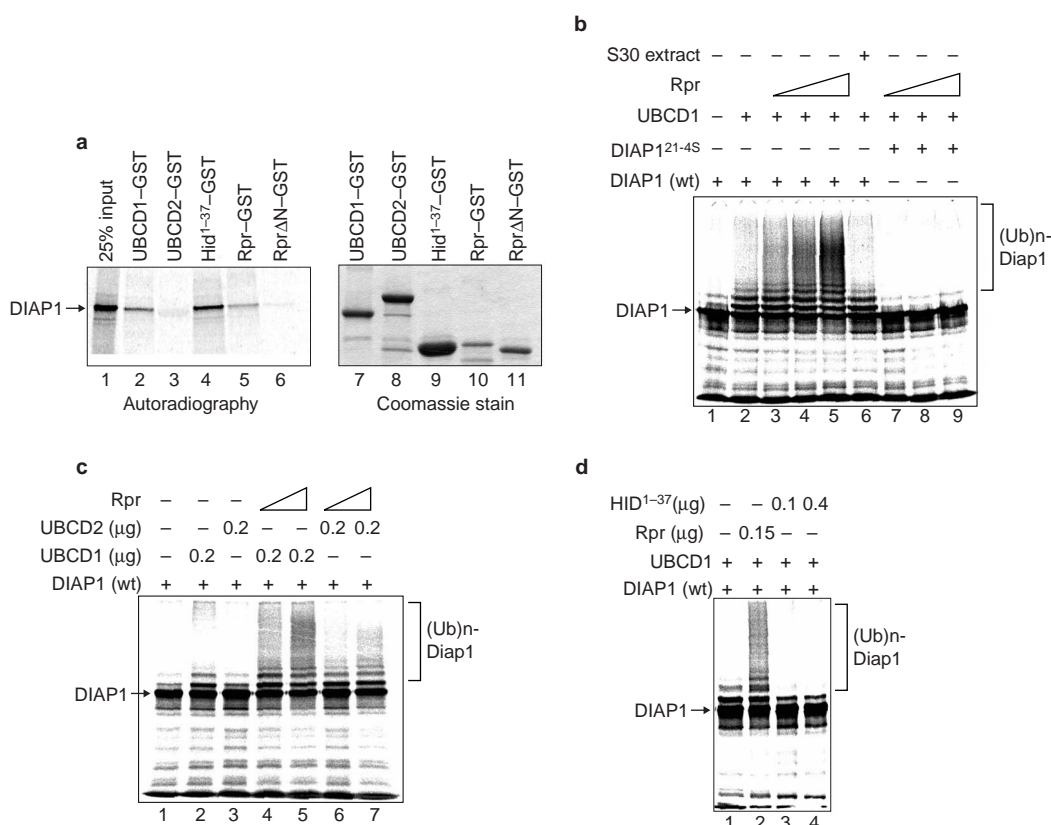
Figure 5 **Rpr and UBCD1 bind DIAP1 and promote DIAP1 auto-ubiquitination *in vitro*. a**, DIAP1 physically interacts with UBCD1, Hid and Rpr. 25% of the input $^{35}$S-DIAP1 was directly loaded in lane 1. The physical interaction between $^{35}$S-DIAP1 and various GST fusion proteins were tested, and retention of $^{35}$S-DIAP1 was visualized by autoradiography (lane2–6). The amount of GST fusion proteins used as bait was visualized by Coomassie staining (lanes 7–11). **b**, *In vitro* ubiquitination of DIAP1 is promoted by UBCD1, Rpr and the DIAP1 RING domain. Minor ubiquitination of $^{35}$S-DIAP1 was observed in the absence of UBCD1, because of background activity derived from the reticulocyte lysate extract used to translate DIAP1 (lane 1). Addition of UBCD1 moderately stimulated the appearance of a ladder-like higher molecular weight species, indicative of DIAP1 polyubiquitination (lane 2). Increasing

amounts of *in vitro* translated Rpr–GST stimulated DIAP1 polyubiquitination in a dose-dependent manner (lane 3–5). In contrast, S30 extract alone did not stimulate DIAP1 ubiquitination (lane 6). DIAP1$^{21-4S}$ was not ubiquitinated at all, even in the presence of UBCD1 and Rpr (lane 7–9). **c**, UBCD2 induces a weaker stimulation of DIAP1, compared to UBCD1. When an identical amount was added, UBCD1 stimulated DIAP1 ubiquitination four to sixfold (lanes 2,4,5), compared to UBCD2 (lanes 3,6,7). Lanes 2 and 3 are the comparisons without Rpr, and lanes 4–6 are in the presence of Rpr. **d**, Hid–GST does not stimulate DIAP1 auto-ubiquitination. The basal level of DIAP1 auto-ubiquitination (lane 1) was stimulated by purified Rpr–GST (lane 2). Although Hid–GST strongly binds DIAP1, increasing amounts of Hid–GST did not stimulate DIAP1 auto-ubiquitination (lanes 3 and 4).

may be an additional target for *ubcD1*-mediated ubiquitination and degradation. Taken together, these genetic interaction assays suggest that UBCD1 is an E2 ubiquitin ligase for DIAP1.

**UBCD1 and Rpr physically interact with DIAP1 *in vitro*.** Ubiquitin ligases physically interact with their cognate ubiquitin-conjugating enzymes to transfer ubiquitin to their substrates. To test if UBCD1 directly interacts with DIAP1, we carried out a glutathione *S*-transferase (GST) pull-down assay with $^{35}$S-methionine-labelled DIAP1. Consistent with a function for UBCD1 as an E2 ubiquitin ligase for DIAP1, $^{35}$S-DIAP1 was retained by UBCD1–GST (Fig. 5a, lane 2). Interestingly, UBCD2, a ubiquitin-conjugating enzyme with high sequence similarity to UBCD1, did not bind DIAP1 in our assay (Fig. 5a, lane 3). These results demonstrate that the UBCD1–DIAP1 interaction is specific, and consistent with our observation where *ubcD1*, but not *ubcD2*, genetically interacts with GMR-*rpr* (Table 1).

The observed affinity between UBCD1–GST and DIAP1 was comparable to the reported interaction between DIAP1 and Hid$^{1-37}$–GST or Rpr–GST[5,6] (Fig. 5a, lanes 4,5). RprΔN–GST, which lacks the RHG motif at the N terminus, bound poorly to DIAP1 (Fig. 5a, lane 6). We conclude that DIAP1 interacts specifically with Rpr, Hid and UBCD1 *in vitro*.

**UBCD1 promotes auto-ubiquitination of DIAP1 *in vitro*.** To determine if DIAP1 auto-ubiquitination is directly mediated by UBCD1, we reconstituted the ubiquitination reaction *in vitro* using recombinant E1, UBCD1 and $^{35}$S-labelled DIAP1. Ubiquitination of DIAP1 was assayed by the appearance of higher molecular weight bands on SDS–polyacrylamide gel electrophoresis (PAGE) gels. Minor ubiquitination of $^{35}$S-DIAP1 was observed in the absence of UBCD1, caused by basal ubiquitin-conjugating enzyme activity in reticulocyte lysates (Fig. 5b, lane 1). The addition of UBCD1 moderately stimulated polyubiquitin chain formation on $^{35}$S-DIAP1 (Fig. 5b, lane 2). When *in vitro* translated Rpr–GST was added to the reaction in increments, stronger DIAP1 ubiquitinating activity was observed (Fig. 5b, lanes 3–5). Such stimulation was not caused by any background activity in the S30 extract itself, where Rpr–GST was translated (Fig. 5b, lane 6).

To examine if DIAP1 itself was the source of the ubiquitin ligase activity, the reaction was repeated with $^{35}$S-DIAP1$^{21-4S}$, which has an inactivating mutation in the RING domain[27]. $^{35}$S-DIAP1$^{21-4S}$ was not ubiquitinated by UBCD1 and Rpr (Fig. 5b, lanes 5–8). These results demonstrate that UBCD1 physically and functionally interacts with the DIAP1 RING domain for DIAP1 auto-ubiquitination, and Rpr stimulates this DIAP1 auto-ubiquitinating activity. Whereas many
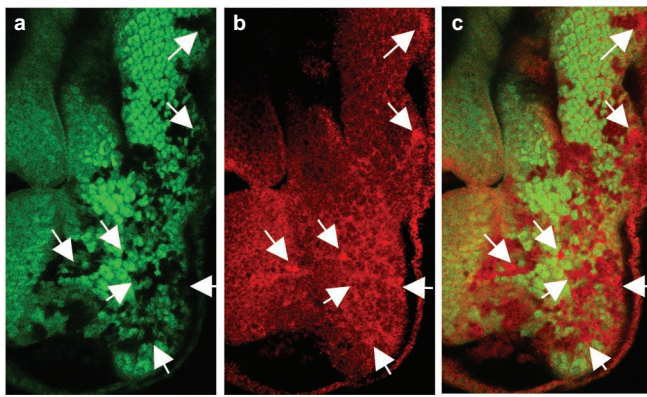
Figure 6 **DIAP1 levels increase in** *ubcD1*^{−/−} **clones.** In all panels, arrows point to representative *ubcD1*^{−/−} clones that have increased anti-DIAP1 labelling. **a**, GFP labelling (green) marks wild type chromosomes. Cells that are not marked with GFP are *ubcD1*^{−/−}. **b**, Anti-DIAP1 labelling (red). **c**, Merged image. All cells that have increased anti-DIAP1 labelling are *ubcD1*^{−/−}.



Figure 7 ***ubcD1*^{−/−} adults have extra-sensory neurons (macrochaetes) in the scutellum. a**, Wild type flies or *UAS-p35* flies invariably have four macrochaetes in the scutellum. **b**, Expression of the *p35* caspase inhibitor results in extra macrochaetes (arrows) in the scutellum. Genotype, *UAS-p35*; *pnr-Gal4*. **c**, Similarly, *trans*-heterozygous *ubcD1*[D112]/*ubcD1*[D73] adults have extra macrochaetes (arrows).
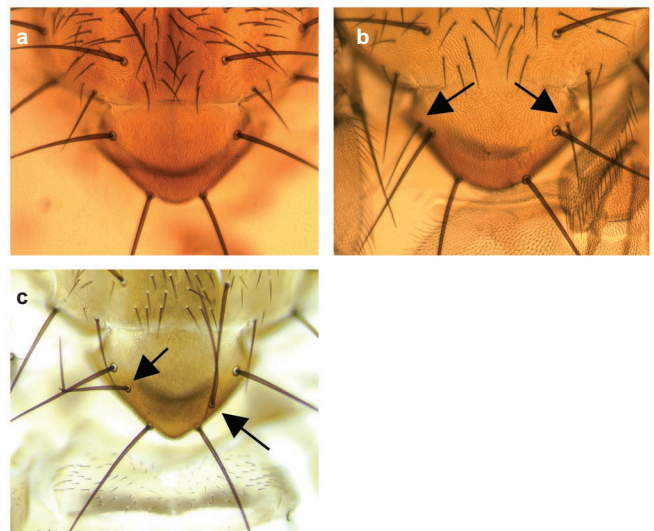
proteins stimulate ubiquitination by bringing ubiquitin ligases in proximity to the substrates, the ability of Rpr to stimulate the ubiquitin ligase activity itself represents a novel mechanism to regulate ubiquitination.

Compared to UBCD1, UBCD2 was significantly less efficient in ubiquitinating DIAP1 *in vitro* (Fig. 5c, lanes 2,3). When the ubiquitinated DIAP1 bands were quantified by phosphorimager, we found that DIAP1 was ubiquitinated four to sixfold less with UBCD2. Likewise, UBCD2 was less efficient in mediating DIAP1 ubiquitination in the presence of Rpr (Fig. 5c, lanes 4–7). These results indicate that UBCD1 shows specificity in promoting DIAP1 ubiquitination *in vitro*, and is consistent with the results from the genetic and physical interaction assays.

We examined if Hid might have a similar stimulating activity for DIAP1 auto-ubiquitination. Whereas purified Rpr–GST stimulated DIAP1 ubiquitination, purified Hid[1–37]–GST, which binds DIAP1 with high affinity (Fig 5a), was not able to stimulate DIAP1 auto-ubiquitination *in vitro* (Fig. 5d). In fact, addition of Hid–GST inhibited the background DIAP1 ubiquitinating activity. This indicates that the stimulation of DIAP1 auto-ubiquitination is not a simple consequence of RHG proteins binding to DIAP1 BIR domain. Furthermore, this *in vitro* assay is consistent with our observation that *hid* does not promote DIAP1 downregulation in wing imaginal discs (Fig. 2).

***ubcD1*^{−/−} cells have higher levels of DIAP1.** To examine the function of *ubcD1* in DIAP1 degradation *in vivo*, we generated mosaic animals with *ubcD1*^{−/−} cells in the context of a largely *ubcD1*^{−/+} animal by using the Flipase/FRT system[36]. Flipase driven with the *eyeless* promoter (*ey-flp*) created small *ubcD1*^{−/−} clones in eye imaginal discs. A subset of *ubcD1*^{−/−} cells labelled more strongly with the anti-DIAP1 antibody, whereas elevated levels of DIAP1 were never detected in wild type cells (Fig. 6). This is consistent with a function of *ubcD1* in promoting DIAP1 degradation.

**Extra cells are observed in *ubcD1*^{−/−} adults.** Each *Drosophila* sensory hair (macrochaete) represents a sensory neuron. *Drosophila* adults have an invariant pattern of sensory cells in the thorax, with four macrochaetes in the scutellum (Fig. 7a). Therefore, the number of macrochaetes has been used as an indicator for defects in cell death or survival[37,38]. The control of apoptosis partly contributes to the regulation of the number of macrochaetes, as expression of *p35* with *panier (pnr)-Gal4* driver results in extra macrochaetes in 30% of animals (*n* = 39; Fig. 7b). *UAS-bcl-2* flies (ref. 38) crossed with *pnr-Gal4* produced similar results (data not shown). Neither of the two parent lines, *pnr-Gal4* nor *uas-p35*, had extra macrochaetes.

We were able to obtain viable adults with a *trans*-hetero-allelic combination of *ubcD1*[D73]/*ubcD1*[D112], albeit with low penetrance. Interestingly, 21% of the surviving adults had extra macrochaete (*n* = 49), similar to *UAS-p35*; *pnr-Gal4* adults (Fig. 7c). Examination of *ubcD1*[598]/*ubcD1*[D112] adults gave similar results (data not shown). These results demonstrate that *ubcD1* affects the number of macrochaetes in adults, and are consistent with a function for *ubcD1* in apoptosis.

***ubcD1* alone is not sufficient to promote DIAP1 degradation.** To test if overexpression of *ubcD1* is sufficient to promote DIAP1 degradation, we overexpressed *ubcd1* in *en-Gal4/UAS-ubcD1* animals. We did not observe any developmental abnormalities in these larvae, as examined during late third instar larval stage (data not shown). DIAP1 protein level remained unchanged in cells expressing *ubcd1*, as compared to its neighbouring control cells of the anterior compartment (data not shown). We conclude that *ubcD1* is not sufficient to promote DIAP1 degradation when expressed on its own. We speculate that additional factors, such as Rpr, may be required to ubiquitinate DIAP1 *in vivo*.

## Discussion

Loss-of-function *diap1* mutants undergo massive apoptosis, whereas overexpression of *diap1* suppresses cell death. Furthermore, a 50% reduction of DIAP1 dosage in *diap1*^{−/+} animals strongly sensitizes cells to apoptosis[3,4,7], indicating that the amount of DIAP1 in a cell determines the threshold to cell death. Here, we demonstrate that the amount of DIAP1 is actively regulated during *Drosophila* development and apoptosis. We observed transcriptional regulation of *diap1* during development and post-transcriptional regulation of DIAP1 during the course of apoptosis. We focused on the post-transcriptional regulation of DIAP1, as it has important conceptual and physiological significance. As apoptosis culminates in morphological changes, including DNA fragmentation, transcriptional regulation would not be an effective means of controlling apoptosis after caspase activation. Furthermore, degradation of IAPs would ensure the irreversibility of the apoptotic process, as it would preclude residual IAP binding to activated caspases. This is

especially important in metazoans, where cell survival after DNA fragmentation can result in the propagation of genetic aberrations that are harmful to the organism.

We find that *rpr* promotes DIAP1 degradation. *Rpr*-mediated DIAP1 degradation is likely to be upstream of caspase activation, as blocking caspases with *p35* maintained the ability of *rpr* to down-regulate DIAP. The following pieces of evidence indicate that *rpr* degrades DIAP1 by ubiquitin-mediated protein degradation. First, whereas DIAP1 is downregulated, the transcription of *diap1-lacZ* is upregulated, precluding the possibility of a transcriptional down-regulation. Second, in *diap1* RING mutant embryos, DIAP1 is not degraded by *rpr*. Third, we are able to reconstitute the DIAP1 auto-ubiquitinating assay *in vitro*. In this assay, the DIAP1 RING domain and E2 ubiquitin ligase activity of UBCD1 is essential for DIAP1 auto-ubiquitination. Interestingly, Rpr is able to stimulate the auto-ubiquitinating activity of DIAP1 *in vitro*. Such stimulating activity of a ubiquitin ligase has not been reported to date and provides a novel mechanism to regulate ubiquitination. Fourthly, UBCD1 is an E2 ubiquitin-conjugating enzyme that genetically and physically interacts with DIAP1. The DIAP1–UBCD1 interaction is specific, as similar ubiquitin-conjugating enzymes, such as UBCD2, do show a genetic or physical interaction with DIAP1. Surprisingly, ectopic *hid* expression produced only a minor effect on DIAP1 levels. Instead, the subcellular distribution of DIAP1 seemed to be modified by *hid*, but remains to be characterized in detail (H.D.R. and H.S. unpublished observations). Consistently, Hid does not stimulate DIAP1 auto-ubiquitination *in vitro*. Taken together, in addition to its DIAP1 binding activity, Rpr has an additional function of stimulating DIAP1 auto-ubiquitination and thereby degrading DIAP1 during apoptosis. As Hid does not stimulate DIAP1 degradation, it is likely that stimulating DIAP1 ubiquitination is not a simple consequence of binding to the DIAP1 BIR domains. Rather, it is likely that Rpr contains a specific motif that mediates its E3-stimulating activity.

Genetic studies on *Drosophila diap1* have previously identified alleles with inactivating mutations in the *diap1* RING domain, which is predicted to specifically abolish its ubiquitin ligase activity[7,27]. These alleles enhanced GMR-*rpr*-induced eye ablation, whereas they suppressed GMR-*hid*. Superficially, these reports seem to be in conflict with a pro-apoptotic function of the DIAP1 RING domain in auto-ubiquitination and self-degradation in response to Rpr. We believe the reason for this apparent discrepancy is probably based on the fact that DIAP1 targets multiple apoptotic regulators for ubiquitination, both pro- and anti-apoptotic, and the genetic interaction assays reflect a mere net effect under a given experimental condition. An accompanying paper, shows that the caspase Dronc is also ubiquitinated by DIAP1, and this seems to contribute to the RING domain mutant phenotype[27]. This can account for the partial loss-of-function phenotype of *diap1* RING alleles, which show excessive apoptosis and die as advanced embryos. Under such conditions, the ability of DIAP1 to ubiquitinate pro-apoptotic proteins seems to override the potential to self-destruct. Nevertheless, this study demonstrates that the ability of DIAP1 to self-degrade in cells that are doomed to die seems to be an important and integral part of apoptosis regulation in *Drosophila*. We propose that Rpr-mediated DIAP1 degradation facilitates apoptosis by removing the 'brake on death', and that it might be possible to exploit this mechanism for therapeutic purposes (see below).

It is interesting to note the parallels between the nature of mammalian thymocyte apoptosis and *Drosophila* metamorphosis. In mammalian thymocytes, IAP degradation can be triggered by glucocorticoids, but the genes that mediate glucocorticoid-induced IAP degradation are not known[19]. During *Drosophila* metamorphosis, the steroid hormone ecdysone triggers larval tissues to undergo apoptosis[40]. Ecdysone receptors activate, among other genes, *rpr* and *hid*, accounting for the cell killing activity of ecdysone[41,42]. Based on such similarity between mammals and

*Drosophila*, we speculate that, in thymocytes, glucocorticoids might activate a Rpr-like protein before IAP degradation and apoptosis. It remains to be determined whether Smac/DIABLO or HtrA2, the only known mammalian RHG proteins to date, promote IAP degradation.

Significantly, the implications from this study may improve our strategies against human pathological conditions, such as cancer. It has been shown that most cancer cells express high levels of IAPs, such as XIAP[43]. At least in some cases, this seems to account for the increased survival ability of tumour cells. We suggest that molecules that combine BIR-binding and E3-ligase-stimulating activities will be useful for the selective reduction of IAP protein levels and may have the potential to selectively kill cancer cells. Although the feasibility of generating small-molecule drugs with such properties remains to be seen, our finding that the 65-amino-acid protein Rpr can stimulate degradation of DIAP1 in *Drosophila* provides a conceptual framework for designing a novel class of anti-cancer drugs. *Note added in proof: Results related to those presented here have been obtained by five other groups and are reported in accompanying papers*[27,50–53]. □

## Methods

### Fly stocks
The following genotypes were used in this study: for ectopic expression of *rpr* or *hid* in the eye, *CyO-2xGMR-rpr / Sco*[44], GMR-hid10 (ref. 45) were used. The *UAS-rpr*; *UAS-p35* and *UAS-hid*; *UAS-p35* lines were generated by crossing *UAS-p35* (ref. 4), *UAS-hid* and *UAS-rpr*[46]. *UAS-dronc*[34], *Pros26*[1], *pbl* TM3 (ref. 28), *st, faf*[BP]/TM6B[29], *ubcD2*[k13206]/CyO[47], *lesswright (lwr)*[47], *uch-L3* (ref. 47), *ubi 63E*[47], *ubcD1*[D73 31], *ubcD1*[D112 31] were used in the genetic interaction assays. *bruce* will be described elsewhere (J. Agapite and H.S., unpublished observations). The *w; FRT*[82B] *ubcD1*[D73] /TM6B line was generated by mitotic recombination. For clonal analysis of *ubcD1*[D73], *ey-flp; FRT*[82B] *Ubi-GFP* was used. For overexpression analyses, GMR-Gal4, *w, en-Gal4, w; prd-Gal4* and *pnr-Gal4* /TM6B[22,48] were used. *th*[5c8] and *wg-lacZ* were used for gene expression analysis[4,49]. *diap1* RING domain mutant alleles are described elsewhere[27]. In brief, *diap1*[33-1S] has a premature stop codon after amino acid 350 and lacks the RING domain. *diap1*[22-8S] has a Cys to Tyr change at amino acid 415, which is within the RING domain.

### Genetic interaction assay
Individual mutants listed in Table 1 were crossed to either GMR-*hid* or GMR-*rpr*, and the eyes of their progeny were compared to unmodified GMR-*hid* or GMR-*rpr*. For unmodified controls, GMR-*hid* or GMR-*rpr* were outcrossed to *canton S*.

### Clonal analysis and overexpression in imaginal discs
Mitotic recombination was induced in the developing eye imaginal discs using the flp-FRT method[36] and *ey-flipase*. The Gal4/UAS system was used for ectopic expression[22].

### Plasmids constructs
The full-length open reading frame (ORF) of *diap1* was subcloned into the *Bam*H1 site of pET14b (Novagen, Madison, WI) to generate the *diap1*[wt]-pET14b expression plasmid. *diap1*[21-4S]-pET14b is identical to *diap1*-pET14b, with the exception of a point mutation in the ORF that converts Cys 406 to Tyr. For His–UBCD1 and His–UBCD2 expression, a full-length ORF was subcloned into the *Bam*H1 site of pET14b. All GST fusion expression plasmids had GST sequence fused in-frame 3′ of a given ORF. UBCD1–GST, UBCD2–GST and Rpr–GST encoded full length ORFs. Hid–GST (a gift from B. Hay) encodes amino acids 1–37 (ref. 6). RprΔN–GST lacks the N-terminal 8-amino-acid residues that constitute the RHG motif. For overexpression of *ubcD1* in flies, a nine-amino-acid haemagglutinin (HA) tag was fused C-terminal to the *ubcD1* ORF. The resulting fusion construct was subcloned into pUAST[22] to generate UbcD1–HA-pUAST. Transgenic flies were subsequently generated by germ line transformation and overexpression of UBCD1–HA was confirmed with anti-HA antibody staining.

### Antibodies, immunohistochemistry and western blots
GST–DIAP1 (ref. 6) was expressed in BL21 (pLysS) *Escherichia coli*, and was gel purified before immunizing rabbits (Cocalico Biologicals, Reamstown, PA). *diap1*[wt]-pET14b was used to express His–DIAP1 in BL21(pLysS) *E. Coli* and was purified according to the manufacturer's protocol (Novagen) before immobilization on nitrocellulose paper to affinity purify anti-DIAP1 antisera. The rabbit anti-β-galactosidase antibody (Cappel, ICN, Costa Mesa, CA), mouse-anti-β-galactosidase antibody (Sigma, St Louis, MO), monoclonal anti-Engrailed antibody (Developmental Studies Hybridoma Bank, Iowa City, IA), Rabbit CM1 antibody[24] and mouse anti-HA antibody (Babco, Denver, PA) were used to stain embryos and imaginal discs under standard conditions. For western blots, 6–18-h-old embryos were homogenized in the lysis buffer (20 mM Tris-HCl at pH 7.5, 100 mM sodium chloride, 1% NP-40 and 2 mM dithiothreitol) and the cell debris was spun down. The supernatant was run on 15% SDS–PAGE gels, transferred to nitrocellulose sheets and probed with the rabbit anti-DIAP1 antibody. Detection was performed by ECL (Amersham Biosciences, Piscataway, NJ).

### GST pull-down assays
[35]S-methionine labelled DIAP1 was generated in an *in vitro* transcription–translation system

# articles

(Novagen) from *diap1*-pET14b. GST fusion plasmids were expressed in BL21(pLysS) cells and extracts were incubated with glutathione–agarose beads to generate various protein–agarose beads. ^{35}S-DIAP1 was incubated with the respective protein–agarose beads overnight at 4 °C in binding buffer (20 mM Tris-HCl at pH 7.5, 150 mM sodium chloride and 0.5% NP-40). The beads were subsequently washed four times with the binding buffer, eluted with sample buffer and analysed on 12% SDS–PAGE gels. ^{35}S-DIAP1 was visualized by Phosphorimaging, and the GST fusion proteins were visualized by Coomassie staining.

## *In vitro* ubiquitination reaction

[35]S-methionine-labelled mutant and wild-type DIAP1 was generated in an *in vitro* transcription–translation system (Promega, Madison, WI) from *diap1*-pET14b and *diap1[121–45]*-pET14b plasmids. For purification of His–UBCD1, *ubcd1*-pET14b was expressed in BL21 (pLysS) *E. coli* and purified on a nickel column in accordance with manufacturer's protocol (Novagen). *In vitro* ubiquitination assays were carried out in a total volume of 20 μl and contained; ^{35}S-methionine-labelled wild-type or mutant DIAP1 (approximately 10,000 cpm), and 250 ng E1 (made in baculovirus; the vector is a kind gift of K. Iwai, University of Osaka, Osaka, Japan). Unless otherwise stated, 1.2 mg His–UBCD1 was used in each reaction. The reaction mixture contained also 40 mM Tris-HCl at pH 7.6, 5 mM magnesium chloride, 1 mM dithiothreitol, 5 mg ubiquitin, 100 ng ubiquitin–aldehyde, 2 mM ATP-γS [Adenosine 5′-O-(3-thiotriphosphate)]. Reactions were incubated for 50 min at 37 °C before addition of sample buffer and resolution on 10% SDS–PAGE gels. Gels were dried and proteins visualized by Phosphorimaging (Fuji, Tokyo, Japan).

1. Jacobson, M. D., Weil, M. & Raff, M. C. Programmed cell death in animal development. *Cell* **88**, 347–354 (1997).
2. Hengartner, M. O. The biochemistry of apoptosis. *Nature* **407**, 685–687 (2000).
3. Goyal, L. Cell death inhibition: keeping caspases in check. *Cell* **104**, 805–808 (2001).
4. Hay, B. A., Wassarman, D. A. & Rubin, G. M. *Drosophila* homologs of baculovirus inhibitor of apoptosis proteins function to block cell death. *Cell* **83**,1253–1262 (1995).
5. Wang, S. L., Hawkins, C. J., Yoo, S. J., Muller, H. A. & Hay, B. A. The *Drosophila* caspase inhibitor DIAP1 is essential for cell survival and is negatively regulated by HID. *Cell* **98**, 453–463 (1999).
6. Goyal, L., McCall, K., Agapite, J., Hartwieg, E. & Steller, H. Induction of apoptosis by *Drosophila reaper*, *hid* and *grim* through inhibition of IAP function. *EMBO J.* **19**, 589–597 (2000).
7. Lisi, S., Mazzon, I. & White, K. Diverse domains of THREAD/DIAP1 are required to inhibit apoptosis induced by REAPER and HID in *Drosophila*. *Genetics* **154**, 669–678 (2000).
8. Wu, J. W., Cocina, A. E., Chai, J., Hay, B. A. & Shi, Y. Structural analysis of a functional DIAP1 fragment bound to grim and hid peptides. *Mol. Cell* **8**, 95–104 (2001).
9. White, K., Grether, M. E., Abrams, J. M., Young, L., Farrell, K. & Steller, H. Genetic control of programmed cell death in *Drosophila*. *Science* **264**, 677–683 (1994).
10. Du, C., Fang, M., Li, Y., Li, L. & Wang, X. Smac, a mitochondrial protein that promotes cytochrome c-dependent caspase activation by eliminating IAP proteins. *Cell* **102**, 33–42 (2000).
11. Verhagen, A. *et al.* Identification of DIABLO, a mammalian protein that promotes apoptosis by binding to and antagonizing IAP proteins. *Cell* **102**, 43–54 (2000).
12. Hegde, R. *et al.* Identification of Omi/HtrA2 as a mitochondrial apoptotic serine protease that disrupts IAP-caspase interaction. *J. Biol. Chem.* **277**, 432–438 (2002).
13. Martins, L. M. *et al.* The serine protease Omi/HtrA2 regulates apoptosis by binding XIAP through a Reaper-like motif. *J. Biol. Chem.* **277**, 439–444 (2002).
14. Suzuki, Y. *et al.* A serine protease, HtrA2, is released from the mitochondria and interacts with XIAP, inducing cell death. *Mol. Cell* **8**, 613–621 (2001).
15. Verhagen, A. *et al.* HtrA2 promotes cell death through its serine protease activity and its ability to antagonise inhibitor of apoptosis proteins. *J. Biol. Chem.* **277**, 445–454 (2001).
16. Joazeiro, C. A. & Weissman, A. M. RING finger proteins: mediators of ubiquitin ligase activity. *Cell* **102**, 549–552 (2000).
17. Huang, H. K. *et al.* The inhibitor of apoptosis, cIAP2, functions as a ubiquitin protein ligase and promotes in vitro monoubiquitination of caspase 3 and 7. *J. Biol. Chem.* **275**, 26661–26664 (2000).
18. Suzuki, Y., Nakabayashi, Y. & Takahashi, R. Ubiquitin-protein ligase activity of X-linked inhibitor of apoptosis protein promotes proteasomal degradation of caspase-3 and enhances its anti-apoptotic effect in Fas-induced cell death. *Proc. Natl Acad. Sci. USA* **98**, 8662–8667 (2001).
19. Yang, Y., Fang, S., Jensen, J. P., Weissman, A. M. & Ashwell, J. D. Ubiquitin protein ligase activity of IAPs and their degradation in proteasomes in response to apoptotic stimuli. *Science* **288**, 874–877 (2000).
20. Blair, S. S. Mechnisms of compartment formation: evidence that non-proliferating cells do not play a critical role in defining the D/V lineage restriction in the developing wing of *Drosophila*. *Development* **119**, 339–351 (1993).
21. Clem, R. J., Fechheimer, M. & Miller, L. K. Prevention of apoptosis by a baculovirus gene during infection of insect cells. *Science* **254**, 1388–1390 (1991).
22. Brand, A. H. & Perrimon, N. Targeted gene expression as a means of altering cell fates and generating dominant phenotypes. *Development* **118**, 401–415 (1993).
23. Baker, N. E. & Yu, S. Y. The EGF receptor defines domains of cell cycle progression and survival to regulate cell number in the developing *Drosophila* eye. *Cell* **104**, 699–708 (2000).
24. Srinivasan, A. *et al. In situ* immunodetection of activated caspase-3 in apoptotic neurons in the developing nervous system. *Cell Death Differ.* **5**, 1004–1016 (1998).
25. Bergmann, A., Agapite, J., McCall, K. & Steller, H. The *Drosophila* gene *hid* is a direct molecular target of Ras-dependent survival signaling. *Cell* **95**, 331–341 (1998).
26. Kurada, P. & White, K. Ras promotes cell survival in *Drosophila* by downregulating *hid* expression. *Cell* **95**, 319–329 (1998).
27. Wilson, P. *et al.* The RING finger of DIAP1 is essential for regulating apoptosis. *Nature Cell Biol.* DOI: 10.1038/ncb799.
28. Saville, K. J. & Belote, J. M. Identification of an essential gene, *l(3)73Ai*, with a dominant temperature-sensitive lethal allele, encoding a *Drosophila* proteasome subunit. *Proc. Natl Acad. Sci. USA* **90**, 8842–8846 (1993).
29. Fischer-Vize, J. A., Rubin, G. M. & Lehmann, R. The *fat facets* gene is required for *Drosophila* eye and embryo development. *Development* **116**, 985–1000 (1992).
30. Treier, M., Seufert, W. & Jentsch, S. *Drosophila* UbcD1 encodes a highly conserved ubiquitin conjugating enzyme involved in selective protein degradation. *EMBO J.* **11**, 367–372 (1992).
31. Cenci, G. *et al. ubcD1*, a *Drosophila* ubiquitin-conjugating enzyme required for proper telomere behaviour. *Genes Dev.* **11**, 863–875 (1997).
32. Neufeld, T. P., Tang, A. H. & Rubin G. M. A genetic screen to identify components of the *sina* signaling pathway in *Drosophila* eye development. *Genetics* **148**, 277–286 (1998).
33. Matuschewski, K., Hauser, H. P., Treier, M. & Jentsch, S. Identification of a novel family of ubiquitin-conjugating enzymes with distinct amino-terminal extensions. *J. Biol. Chem.* **271**, 2789–2794 (1996).
34. Meier, P., Silke, J., Leevers, S. J. & Evan, G. I. The *Drosophila* caspase DRONC is regulated by DIAP1. *EMBO J.* **19**, 598–611 (2000).
35. Quinn, L. M. *et al.* An essential role for the caspase *dronc* in developmentally programmed cell death in *Drosophila*. *J. Biol. Chem.* **275**, 40416–40424 (2000).
36. Xu, T. & Rubin, G. M. Analysis of genetic mosaics in developing and adult *Drosophila* tissues. *Development* **117**, 1223–1237 (1993).
37. Kanuka, H. *et al.* Control of the cell death pathway by *Dapaf-1*, a *Drosophila* Apaf-1/CED-4-related caspase activator. *Mol. Cell* **4**, 757–769 (1999).
38. Rodriguez, A. *et al. Dark* is a *Drosophila* homologue of Apaf-1/CED-4 and functions in an evolutionarily conserved death pathway. *Nature Cell Biol.* **1**, 272–279 (1999).
39. Gaumer, S., Guenal, I., Brun, S., Theodore, L. & Mignotte, B. bcl-2 and bax mammalian regulators of apoptosis are functional in *Drosophila*. *Cell Death Differ.* **7**, 804–814 (2000).
40. Baehrecke, E. H. Steroid regulation of programmed cell death during *Drosophila* development. *Cell Death Differ.* **7**, 1057–1062 (2000).
41. Lee, C. Y. *et al. E93* directs steroid-triggered programmed cell death in *Drosophila*. *Mol. Cell* **6**, 433–443 (2000).
42. Jiang C., Lamblin, A. F., Steller H. & Thummel C. S. A steroid-triggered transcriptional hierarchy controls salivary gland cell death during *Drosophila* metamorphosis. *Mol. Cell* **5**, 445–455 (2000).
43. Tamm *et al.* Expression and prognostic significance of IAP-family genes in human cancers and myeloid leukemias. *Clin. Cancer Res.* **6**, 1796–1803 (2000).
44. White, K., Tahaoglu, E., Steller, H. Cell killing by the *Drosophila* gene *reaper*. *Science* **271**, 805–807 (1996).
45. Grether, M. E., Abrams, J. M., Agapite, J., White, K. & Steller, H. The head involution defective gene of *Drosophila melanogaster* functions in programmed cell death. *Genes Dev.* **9**, 1694–1708 (1995).
46. Zhou, L. *et al.* Cooperative functions of the *reaper* and *head involution defective* genes in programmed cell death of *Drosophila* CNS midline cells. *Proc. Natl Acad. Sci. USA* **94**, 5131–5136 (1997).
47. Spradling, A. C. *et al.* The Berkeley *Drosophila* Genome Project gene disruption project: Single P-element insertions mutating 25% of vital *Drosophila* genes. *Genetics* **153**, 135–177 (1999).
48. Calleja, M. & Morata, G. Visualization of gene expression in living adult *Drosophila*. *Science* **274**, 252–255 (1996).
49. Cohen, B., Simcox, A. A. & Cohen, S. M. Allocation of the thoracic imaginal primordia in the *Drosophila* embryo. *Development* **117**, 597–608 (1993).
50. Holley, C.L., Olson, M.R., Colon-Ramos, D.A. & Kornbluth S. Reaper eliminates IAP proteins through stimulated IAP degradation and generalized translational inhibition. *Nature Cell Biol.* DOI: 10.1038/ncb798.
51. Hays, R., Wickline, L. & Cagan, R. Morgue mediates apoptosis in the *Drosophila melanogaster* retina by promoting degradation of DIAP1. *Nature Cell Biol.* DOI: 10.1038/ncb794.
52. Wing *et al. Drosophila* Morgue is a novel F box/ubiquitin conjugase domain protein important for *grim-reaper*-mediated apoptosis. *Nature Cell Biol.* DOI: 10.1038/ncb800.
53. Yoo *et al.* Hid, Rpr and Grim negatively regulate DIAP1 levels through distinct mechanisms. *Nature Cell Biol.* DOI: 10.1038/ncb793.

COMPETING FINANCIAL INTERESTS
The authors declare that they have no competing financial interests.

# errata

In Ryoo *et al.* (*Nature Cell Biology*, **4,** 432–438 (2002)), Table 1 (shown below) was omitted from both the print and online versions.

| Table 1 Genetic interaction assay with GMR-*hid* and GMR-*rpr*. | |
| --- | --- |
| **No modification** | *ubcD2* (ubc4 homolog), *lesswright* (ubc9), *ubi 63E* (ubiquitin), *uch-L3* (deubiquitinating enzyme), *seven in absentia* (*sina*) |
| **Enhancer of GMR-*rpr*** | *Pros26* (Proteasome subunit), *fat facet* (deubiquitinating enzyme) *bruce* (mod86) |
| **Suppressor of GMR-*hid,* GMR-*rpr*** | *ubcD1* (alleles D73 and 598) |

In the Discussion section of the same paper (page 437, line 17 of the second paragraph), the word 'not' is missing from the following sentence: 'The DIAP1–UBCD1 interaction is specific, as similar ubiquitin-conjugating enzymes, such as UBCD2, do not show a genetic or physical interaction with DIAP1.'

These changes have also been made to the online version of the manuscript.

# errata

In Ryoo *et al.* (*Nature Cell Biology*, **4**, 432–438 (2002)), Table 1 (shown below) was omitted from both the print and online versions.

| Table 1 Genetic interaction assay with GMR-*hid* and GMR-*rpr*. | |
|---|---|
| **No modification** | *ubcD2* (ubc4 homolog), *lesswright* (ubc9), *ubi 63E* (ubiquitin), *uch-L3* (deubiquitinating enzyme), *seven in absentia* (*sina*) |
| **Enhancer of GMR-*rpr*** | *Pros26* (Proteasome subunit), *fat facet* (deubiquitinating enzyme) *bruce* (mod86) |
| **Suppressor of GMR-*hid*, GMR-*rpr*** | *ubcD1* (alleles D73 and 598) |

In the Discussion section of the same paper (page 437, line 17 of the second paragraph), the word 'not' is missing from the following sentence: 'The DIAP1–UBCD1 interaction is specific, as similar ubiquitin-conjugating enzymes, such as UBCD2, do not show a genetic or physical interaction with DIAP1.'

These changes have also been made to the online version of the manuscript.